

PAPER

Positronium formation at 4H SiC(0001) surfaces

To cite this article: A Kawasuso *et al* 2020 *J. Phys.: Condens. Matter* **33** 035006

View the [article online](#) for updates and enhancements.



IOP | ebooks™

Bringing together innovative digital publishing with leading authors from the global scientific community.

Start exploring the collection—download the first chapter of every title for free.

Positronium formation at 4H SiC(0001) surfaces

A Kawasuso^{1,*}, K Wada¹, A Miyashita¹, M Maekawa¹, H Iwamori², S Iida² and Y Nagashima²

¹ National Institutes for Quantum and Radiological Science and Technology, 1233 Watanuki, Takasaki, Gunma 370-1292, Japan

² Tokyo University of Science, 1-3 Kagurazaka, Shinjuku-ku, Tokyo 162-8601, Japan

E-mail: kawasuso.atsuo@qst.go.jp

Received 2 July 2020, revised 17 September 2020

Accepted for publication 5 October 2020

Published 20 October 2020



Abstract

Positronium formation at 4H SiC(0001) surfaces were investigated upon the removal of natural oxide layers by hydrofluoric acid etching and heat treatment at 1000 K in ultra-high vacuum. Two types of positronium were observed in the positronium time-of-flight (PsTOF) measurements irrespective of conduction type and surface polarity. One type formed the major part of the PsTOF spectrum with a maximum energy of 4.7 ± 0.3 eV. This energy exceeded the theoretical value calculated with valence electrons. The PsTOF spectrum shape was different from those of metal surfaces, suggesting that the surface state electrons or conduction electrons need to be considered as the positronium source. Another positronium appeared at 1000 K in the tail of the PsTOF spectrum with a maximum energy of 0.2–0.5 eV. This thermally-assisted athermal positronium may be formed via the surface state positrons and electrons.

Keywords: positronium, SiC, surface, positron re-emission

(Some figures may appear in colour only in the online journal)

1. Introduction

Positronium, the bound state of an electron and a positron [1, 2], has been extensively investigated in fundamental physics [3–5]. Positronium is also expected to be a unique probe for surface electronic states because the energy and momentum distributions of positronium formed at a solid surface reflect the surface band structure [6, 7]. Therefore, understanding positronium formation at solid surfaces is important.

There are three main positronium formation mechanisms at metal and semiconductor surfaces: (i) the direct formation at surface with negative formation potential, (ii) the surface positron-mediated mechanism, and (iii) the energetic positron scattering mechanism [8, 9].

However, at semiconductor surfaces, some special characteristics, such as the band gap, low free electron density, and surface dangling bond states, must be considered. More plainly speaking, semiconductors are intermediate in

character between metals and insulators. Therefore, at semiconductor surfaces, positronium may be ejected via the excitonic (or quasi-positronium) precursor state, which is nearly impossible in metals and analogous to some insulators where positronium is emitted from inside to the vacuum [10].

Over the last decade, the UCR group examined positronium formation at Si and Ge surfaces [11, 12]. Based on positronium time-of-flight (PsTOF) spectroscopy, we found strong doping and temperature dependences of positronium formation processes at Si surfaces [13]. The positron work functions of Si and Ge are positive, and hence positrons are confined inside and in the surface mirror potentials. Whereas, the other group IV semiconductors, SiC and diamond, have negative positron work functions [14, 15]. It is therefore important to investigate the positronium formation at such semiconductor surfaces.

In this paper, we investigated the positronium formation at 4H SiC(0001) surfaces using PsTOF spectroscopy. The maximum kinetic energy of positronium was considerably greater than that expected from theory and was independent of conduction type and surface polarity.

* Author to whom any correspondence should be addressed.

2. Experiment

The samples were modified Lely-grown n- and p-type 4H SiC(0001) and n-type 4H SiC(000 $\bar{1}$) purchased from Cree Research Inc. The room temperature resistivities were 0.1 Ω cm (n-type) and 3 Ω cm (p-type). To remove the native oxide layers, the samples were dipped in 50% hydrofluoric acid for 5 min and cleaned with ultrapure water. The samples were further cleaned by heating at 1000 K in a vacuum (base pressure: 10^{-7} – 10^{-8} Pa).

First, the positron work functions were determined from the positron re-emission measurements at 300 K using a source-based $E \times B$ type positron beam with an energy of $E_+ = 3$ keV and a conventional retarding grid in front of sample [16]. The positron re-emission efficiency was obtained from the change of 511 keV gamma ray counts measured by a high-purity Ge detector with the calibration considering the positronium fraction.

The positronium fractions were determined at 10–1000 K through the annihilation gamma ray energy measurements with a high-purity Ge detector and a magnetically guided positron beam as $I_{Ps} = 1/[1 + (P_{100\%}/P_{0\%})(R_{100\%} - R)/(R - R_{0\%})]$, where P is the two-gamma intensity at 511 keV, R is the three-gamma intensity below 511 keV, the subscript denotes the 100(0)% positronium intensity determined from measurements of Ge(111) at 1000 K and mica at 300 K [17–19]. The further details are described elsewhere [13].

The PsTOF measurements were carried out at 300–1000 K at the Slow Positron Facility of the High Energy Acceleration Research Organization in Japan [20, 21]. The beam energy was $E_+ = 3$ or 4.2 keV. The average open angle of detectable positronium was 26° to the surface normal. The horizontal length between the sample and the detector slit centers (L) was 40 or 120 mm. The width (d) and length (D) of slit, and the beam pipe radius (R) were 6 mm, 100 mm and 125 mm, respectively. The above horizontal lengths were then effectively $L_{\text{eff}} = L - d(1/2 + R/D) = 30$ and 110 mm. The time to energy conversion was made with these effective lengths. The time resolution of the electronic system was approximately 10 ns in the full width of the prompt peak. The spectrum threshold times were determined by taking into account of this time resolution. The time resolution function was approximated by a Gaussian function with the width at 1/10 maximum between the earliest and latest detection times of positronium at the slit ($t_{e,l} = [L_{\text{eff}}D \mp d(1/2 + R/D)]/\sqrt{E/m} \mp 5$ ns, where E is the positronium kinetic energy and m is the electron rest mass) and a factor of $t^2 \exp(t/142$ ns) for monoenergetic positronium ejected perpendicularly from the surface. Then, by converting the time scale to the energy scale, the energy resolution was obtained. A typical energy resolution is ~ 0.5 eV for $E = 3$ eV and it becomes better (worse) with increasing (decreasing) E . This analytical estimation was further confirmed by a Monte Carlo simulation assuming the above geometrical conditions.

3. Results

Figure 1 shows the positron re-emission spectra and their derivatives obtained for the n- and p-type (0001) surfaces as

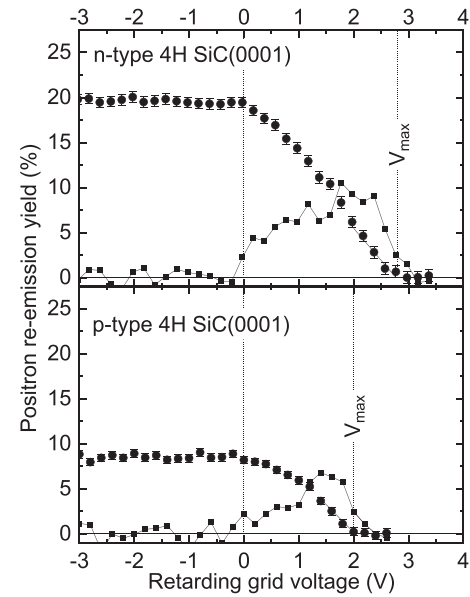


Figure 1. Positron re-emission spectra (filled circles) and their derivatives (filled squares) obtained for n- and p-type 4H SiC(0001) surfaces at 300 K as a function of retarding grid voltage in front of the sample. The incident positron beam energy is 3 keV.

a function of the retarding grid voltage relative to the sample. When the retarding grid voltage is negative, the re-emitted positrons are extracted from the sample towards the grid, producing the constant re-emission yield. In contrast, as the retarding grid voltage increases, the re-emitted positrons are pushed back to the sample, and hence the re-emission yield decreases. The maximum energy of re-emitted positrons is obtained by the retarding grid voltage at which the re-emission yield is zero, as denoted by V_{max} in figure 1. The maximum energies are 2.8 ± 0.2 eV for the n-type surface and 2.0 ± 0.4 eV for the p-type surface. The re-emission yield for the n-type surface is more than twice that for the p-type surface. The derivatives of spectra show that the reemitted positrons have wide energy distributions from zero to the maximum energies. Thus, both the re-emission energy and yield are different for n- and p-type surfaces.

Figure 2 shows the PsTOF spectra obtained for the n- and p-type (0001) surfaces and the n-type (000 $\bar{1}$) surface at 300 K and 1000 K and $L = 120$ mm on the same vertical scale. The lifetime backgrounds ($\propto \exp(-t/142$ ns)) created by the Compton-scattered gamma rays of in-flight ortho-positronium annihilation are subtracted. At 300 K, the spectrum shapes are similar for all the surfaces. The maximum positronium energy is determined to be $E_{\text{max}} = 4.7 \pm 0.3$ eV. We call this positronium ‘type A’. The intensity of type A positronium for the p-type surface increases at 1000 K, whereas for the n-type (0001) surface, the tail intensity increases at 1000 K. The tail component is clearer in the inset figures obtained at $L = 40$ mm. This component is weak for the p-type (0001) and n-type (000 $\bar{1}$) surfaces, but not completely absent as seen in the inset figures. The maximum kinetic energy is ~ 0.5 eV for the (0001) surfaces and ~ 0.2 eV for the (000 $\bar{1}$) surface. We call this positronium ‘type B’.

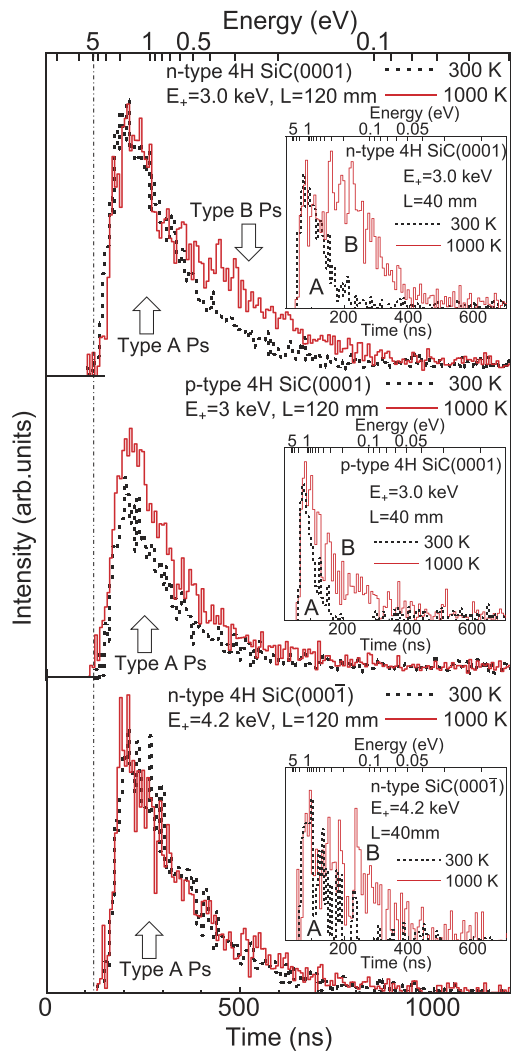


Figure 2. Positronium time-of-flight spectra obtained for n- and p-type 4H SiC(0001) surfaces and n-type 4H SiC(000 $\bar{1}$) surface at 300 K (broken lines) and 1000 K (solid lines) and at $L = 120$ mm. The dashed-dotted line denotes the spectrum threshold position. The insets are the spectra obtained at $L = 40$ mm.

Figure 3 shows the temperature dependence of the positronium fraction obtained for the n- and p-type (0001) and n-type (000 $\bar{1}$) surfaces. There is no distinct hysteresis behavior in the cooling and heating runs. For the (000 $\bar{1}$) surface, the positronium fraction is severely degraded below ~ 100 K, probably due to the gas adsorption (data not shown) [22]. For the n-type (0001) surface, the positronium fraction increases in two steps, the first from 100 to 500 K and the second above 700 K. The second increase probably corresponds to the appearance of the type B positronium seen in figure 2. For the p-type (0001) surface, the positronium fraction increases monotonically above 100 K and tends to saturate above 700 K. For the n-type (000 $\bar{1}$) surface, after the common increase above 100 K, the positronium fraction is almost constant from 400 to 1000 K. In the latter two cases, as shown in figure 2, the intensities of type B positronium are low, and hence their appearances are not apparently seen as the increments of positronium fractions at high temperatures in figure 3.

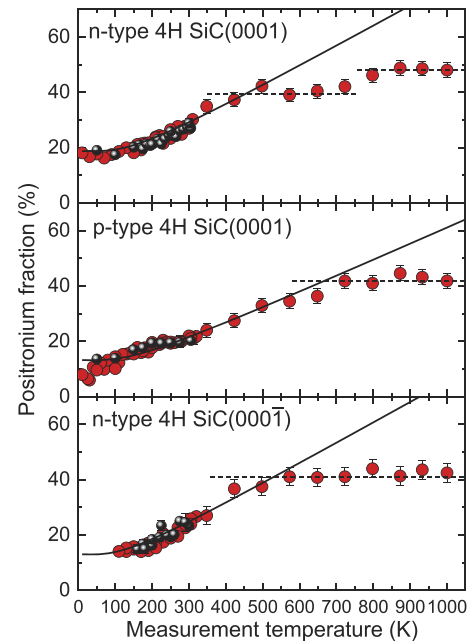


Figure 3. Temperature dependence of positronium fraction obtained for n- and p-type 4H SiC(0001) and n-type 4H SiC(000 $\bar{1}$) from 10 to 1000 K. Red and black circles denote data obtained in the cooling and heating runs, respectively. The solid lines denote the theoretical expectation based on the phonon-mediated process.

4. Theoretical calculation

To interpret the experimental data, we performed the density functional theory calculation for 4H SiC(0001) using the ABINIT [23] with the projector augmented-wave method [24] within the generalized gradient approximation (GGA) [25]. The electron–positron correlation energy functional was based on the GGA method [26]. The positronium formation potential was determined as $\Phi_{Ps} = -A_+ - 6.8$ eV, where A_+ is the positron affinity, using the primitive cell with full structural optimization and k -point sampling of $12 \times 12 \times 4$. The positron work function was determined by $\phi_+ = -A_+ + \phi_-$, where ϕ_- is the electron work function calculated by a slab crystal of eight bilayers in the surface normal direction with the primitive cell in the surface parallel direction, with k -point sampling of $12 \times 12 \times 1$. The (0001) surface was bulk-truncated, and the (000 $\bar{1}$) surface was terminated with H atoms. The initial vacuum layer was 20 Å. For positrons, only the Γ point was considered. The positron surface state was also calculated with a corrugated mirror potential implemented as the surface potential for positrons [27–30]. The valence electron configurations were $2s^2 2p^6 3s^2 3p^2$ (Si) and $2s^2 2p^2$ (C). Table 1 lists the results of the calculation. Both positron work function and positronium formation potential are negative, suggesting spontaneous emission. The positron surface state is also formed. The positronium formation potentials based on the bulk calculation and the slab calculation coincide suggesting the self-consistency of the calculation. The positron affinity is in good agreement with the previous report [31]. The positron work function also agrees with the experimental values determined so far [32–35].

Table 1. Calculated positron affinity(A_+), positronium formation potential (Φ_{Ps}), electron and positron work functions(ϕ_- , ϕ_+), surface dipole barrier(Δ_{SD}) and surface positron binding energy(E_B) for 4H SiC(0001) surface in eV.

Bulk calculation		Slab calculation				
A_+	Φ_{Ps}	Surface	ϕ_-	ϕ_+	Δ_{SD}	E_B
-4.56	-2.24	(0001)	+6.46	-1.90	+15.08	+2.19

5. Discussion

5.1. Positron re-emission

Previous positron re-emission experiments on SiC(0001) surfaces were performed mostly using n-type SiC with no surface treatments [32–37]. Thus, the surfaces were probably covered with natural oxide layers, although sufficient positron re-emission was observed. This implies that positron re-emission occurs easily at n-type surfaces. On the contrary, positron re-emission at p-type surfaces was reported to be zero [33] or much smaller than that at n-type surfaces [37]. This work supports the efficient positron re-emission at n-type surfaces and shows the efficient positron re-emission at the p-type surface, although the amount is lower than that for the n-type surfaces (figure 1). The maximum energy of re-emitted positrons at n-type surface is 0.8 eV greater than at p-type surface.

The differences in positron re-emission efficiency and the maximum re-emission energy between n- and p-type surfaces are probably explained by band bending near the sub-surface, as shown schematically in figure 4 [38, 39]. In the flat band condition, the positron work function is uniquely determined as ϕ_+^{FB} without depth dependence. However, the opposite band bendings are induced in the n- and p-type sub-surface regions. In n-type surfaces, the positron ground state energy may be raised by Δ from the flat band level, whereas in p-type surfaces the energy may be decreased with a different Δ . Injected positrons tend to move to the surface in n-type sub-surface and to be repelled from the surface in p-type sub-surface, which explains the different positron re-emission yields observed for n- and p-type surfaces.

Even if band bending occurs, if positrons move along the potential plane adiabatically, the maximum energy of re-emitted positrons should be $-\phi_+^{FB}$ in both n- and p-type surfaces. However, in n-type sub-surface, some positrons may get to the surface without losing their energies fully and are re-emitted as epithermal positrons. Conversely, in p-type sub-surface, the energy of positrons getting to the surface may not exceed $-\phi_+^{FB}$. This explains the different maximum energies of re-emitted positrons obtained for n- and p-type surfaces. In this context, $\phi_+^{FB} = -2$ eV from the maximum re-emission energy of positrons for the p-type surface, comparable to the calculated value in the flat band condition (table 1).

5.2. Positronium formation

Type A positronium with $E_{max} = 4.7$ eV is commonly seen for n- and p-type (0001) and n-type (000 $\bar{1}$) surfaces (figure 2). That is, the type A positronium is formed by the same

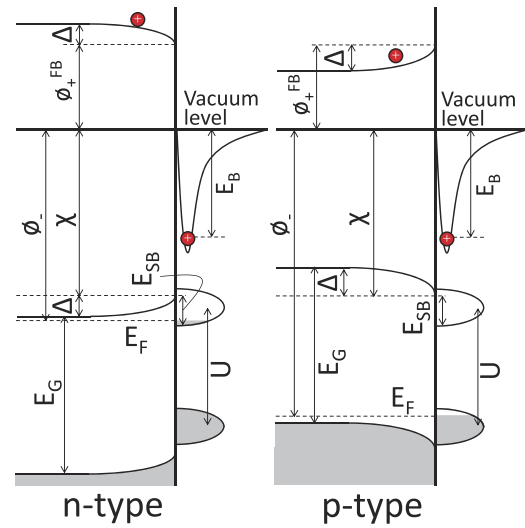


Figure 4. Schematic energy diagrams of positrons and electrons for n- and p-type conditions considering the band bending effect. Δ is the dipole barrier due to the band bending, ϕ_- is the electron work function, χ is the electron affinity, E_G is the band gap, E_F is the Fermi level, U is the Mott–Hubbard energy, E_{SB} is the energy difference between the bottoms of the conduction band and the upper surface band, ϕ_+^{FB} is the positron work function in the flat band condition and E_B is the binding energy of surface positron. Δ and ϕ_- are different between n- and p-type conditions, while the other quantities are common.

mechanism irrespective of conduction type and surface orientation. One may assume that the type A positronium is formed through the direct process at the surface with negative formation potential. However, the maximum kinetic energy ($E_{max} = 4.7$ eV) is substantially larger than that expected from the theory, i.e., $-\Phi_{Ps}^{calc} = 2.24$ eV in table 1. The theory assumes that valence electrons are the source of positronium. Therefore, to explain the observed maximum kinetic energy of type A positronium, we need to consider the other electrons located above the valence band maximum.

First, we consider the case in which positrons pick up surface state electrons during the transmission through the surface to the vacuum. The prerequisites to explain the unique value of $E_{max} = 4.7$ eV are that positrons pick up electrons in the same energy levels and the positron work function is also common, irrespective of conduction type and surface orientation. However, the second prerequisite conflicts with the experimental fact that the positron work function is different for n- and p-type surfaces. It may be assumed that only positrons get to the surface adiabatically, that is, with the flat band work function ($\phi_+^{FB} = -2$ eV), participate in the type A positronium formation in both n- and p-type surfaces. Then, the positronium formation potential is given by $\Phi_{Ps} = -2.0 + \chi + E_{SB} - 6.8$ eV, where χ is the electron affinity (3.7–4.2 eV) and E_{SB} is the energy separation between the bottoms of the surface and conduction bands. If we assume $\Phi_{Ps} = -E_{max} = -4.7$ eV, we have $E_{SB} = -0.1 + 0.4$ eV. Thus, the responsible surface band must be located near the bottom of the conduction band.

On both the (0001) and (000 $\bar{1}$) surfaces, the original metallic bands are likely split into two bands due to the effect of Mott–Hubbard Coulomb repulsion, U (figure 4) [40]. One

band is below the half of the band gap and the other is near the bottom of the conduction band. Without charge transfer, the lower band is filled state and the upper band is empty. In the context of positrons picking up surface state electrons, the upper band electrons are responsible for type A positronium formation. In n-type surfaces, the upper band may be partially filled due to the charge transfer from the bulk, whereas in p-type surfaces, the upper band should be empty and the lower band is further doped with holes. Under the electron excitation by positron impact, the upper bands of p-type surfaces may be partially filled at least temporarily. If so, the unique maximum kinetic energy of type A positronium for n- and p-type surfaces can be explained. However, according to theory [41] and experiment [42], the energy levels of surface bands should be different for the (0001) and (000 $\bar{1}$) surfaces by at least 0.5 eV, and the band widths on the (0001) and (000 $\bar{1}$) surfaces are also different. This is because the surface bands on these two surfaces are associated with Si and C dangling bonds, respectively, and hence are in different electronic states. The unique maximum kinetic energy of type A positronium ($E_{\max} = 4.7$ eV) for the (0001) and (000 $\bar{1}$) surfaces is not readily explained considering the surface state electrons.

We then suppose that conduction electrons are the source of type A positronium. Because the effects of band bending on ϕ_- and ϕ_+ may be opposite, the effects are mutually canceled out. Therefore, the positronium formation potential is uniquely determined irrespective of conduction type and surface polarity. With the energy gain of the band gap (~ 3.2 eV), the theoretical formation potential can be $\Phi_{\text{Ps}}^{\text{cal}} = -2.2 - 3.2 = -5.4$ eV. In addition, assuming $\phi_+^{\text{FB}} = -2$ eV, then $\Phi_{\text{Ps}} = \phi_+^{\text{FB}} + \chi - 6.8 = -5.1 \sim -4.7$ eV. These can explain the maximum kinetic energy of type A positronium ($E_{\max} = 4.7$ eV) within uncertainties. Considering that the number of conduction electrons is limited even in n-type surfaces at thermal equilibrium, the excitation of conduction electrons by positron impact should be considered.

In 4H SiC, the bottom of the conduction band is located at the M point with the transverse wave vector of 1.18 \AA^{-1} , and thus, from the momentum conservation law, the positronium emission angle is $\sim 43^\circ$. This is out of the average aperture acceptance of the PsTOF apparatus ($\sim 26^\circ$) though it is still in the maximum acceptance ($\sim 45^\circ$), most positronium atoms emitted with large angles may collide with the aperture and the beam pipe wall, reducing their in-flight annihilation events. If phonon absorption and/or emission occur in the positronium formation process, the emission angle may be within the average aperture acceptance [43]. These phonon processes may increase with increasing temperature, and the temperature dependence of the positronium fraction is described as being proportional to $\coth[E_{\text{ph}}/(2kT)] + \text{const.}$, where E_{ph} is the phonon energy, k is the Boltzmann constant, and T is temperature. The observed temperature dependence from 100 to 400 K may be described with this function with $E_{\text{ph}} = 50$ meV (figure 3). The deviations from this function at high temperatures probably indicate the upper limits of the positronium fraction due to the available number of positrons reaching the surface. Thus, the explanation for type A positronium formation with conduction electrons may be possible.

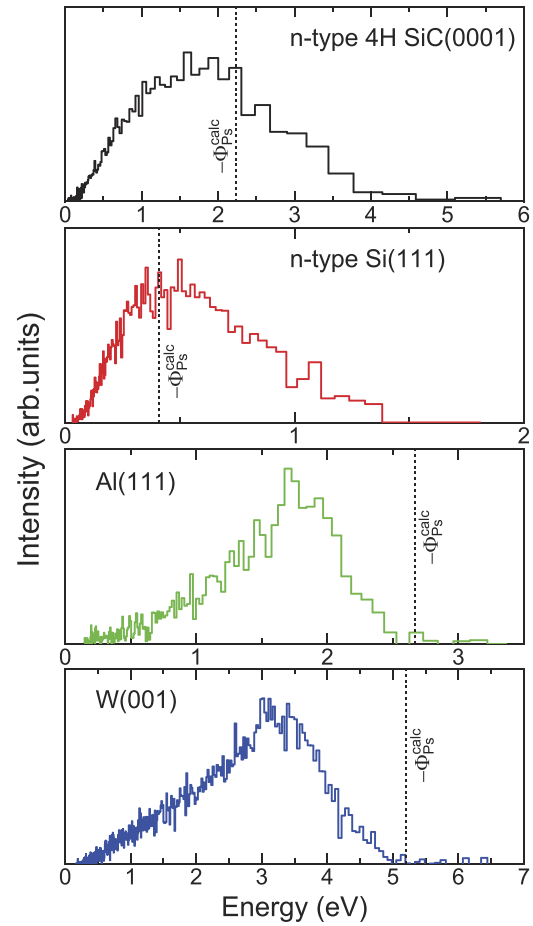


Figure 5. Positronium time-of-flight spectra obtained for n-type 4H SiC(0001), n-type Si(111), Al(111), and W(001) surfaces at 300 K and at $L = 120$ mm in the energy scale. The broken lines denote the positions of theoretical positronium formation potentials.

A discrepancy in maximum positronium energy between experiment and theory has also been reported for Si surfaces as shown in figure 5 [13]. Furthermore, in figure 5, it is interesting to note that the spectra obtained for metallic Al(111) and W(001) surfaces relatively sharply rise near $-\Phi_{\text{Ps}}^{\text{calc}}$ [44], while the spectra of Si and SiC rise gradually at well above $-\Phi_{\text{Ps}}^{\text{calc}}$. In the case of metals, the electrons in the occupied state, i.e., below the Fermi level, are basically picked up by positrons and hence the maximum positronium energy corresponds to the Fermi level. Conversely, the spectra for Si and SiC imply the positronium formation by picking up conduction electrons. To get more direct confirmations about the contribution of conduction electrons, the further experiments are needed. The observations under the band gap excitation by electron bombardment or laser illumination will be feasible [45]. SiC, Si, and Ge are all indirect gap semiconductors. Positronium formation at direct gap semiconductor surfaces is also intriguing.

As mentioned in introduction, an important argument would be, if excitonic (or quasi-positronium) state is already formed between a positron and an electron inside and then it is ejected into the vacuum or a positron and an electron at the surface suddenly form the positronium state in the

vacuum. More apparent example for the former is the positronium emission from insulators [10]. In semiconductors, the excitonic state may be formed inside because of negligible screening by free electrons. However, the large Borh radius and small binding energy due to the dielectric screening makes the detection of excitonic state difficult [46]. In the case of Si, the type A positronium may be explained as the emission from the excitonic state because positrons are confined inside or in the surface potential due to the positive work function. While, the positron work function of SiC is negative and hence the formation of excitonic state inside is not necessarily important, though the binding energy will be larger than that in Si by the smaller dielectric constant and hence the excitonic state will be more stable. The observed maximum kinetic energy of type A positronium ($E_{\max} = 4.7$ eV) should correspond to the positronium work function including the binding energy of excitonic state (30–100 meV) in the former case, while simply to the positronium formation potential in the latter case [47].

Type B positronium is clearly visible in figure 2 for the n-type (0001) surface at 1000 K with a maximum kinetic energy of ~ 0.5 eV and also as an increase in the positronium fraction above 800 K in figure 3. In contrast, for the p-type (0001) and n-type (000 $\bar{1}$) surfaces, type B positronium is rather weak, and hence despite its presence, the increases in positronium fraction are not seen in figure 3. The maximum energy of type B positronium is ~ 0.2 eV for the n-type (000 $\bar{1}$) surface, which is slightly lower than that for the (0001) surface. Type B positronium, that is, the thermally-assisted athermal positronium, is also reported for Si and Ge [11–13]. In previous studies, it has been assumed that type B positronium is formed from surface state positrons and thermally excited surface state electrons. In the case of SiC, the Mott–Hubbard band corresponds to this surface electron state. The maximum kinetic energy may be given by $-E_B - \chi - E_{SB} + 6.8$ eV. Using the theoretical $E_B = 2.2$ eV in table 1 and $E_{SB} = 0.5$ and 1 eV for the (0001) and (000 $\bar{1}$) surfaces, respectively [42], the maximum kinetic energy is estimated to be ~ 0.7 eV for the (0001) surface and ~ 0.2 eV for the (000 $\bar{1}$) surface. These results agree well with the observed values. The formation of type B positronium is less efficient at p-type (0001) and n-type (000 $\bar{1}$) surfaces. For the p-type (0001) surface, this may be explained by the less efficient excitation from the lower to upper bands due to the hole doping to the lower band. For the (000 $\bar{1}$) surface, this may also be explained by the inefficient interband excitation due to the larger U value (~ 2.5 eV) compared with that for the (0001) surface (~ 1.9 eV).

6. Summary

The maximum energies of positrons re-emitted from n- and p-type 4H SiC(0001) surfaces were different, implying the importance of the band bending effect on the positron ground state energy in semiconductors. Two types of positronium were formed at the 4H SiC(0001) surface, irrespective of conduction type and surface polarity. One was formed through the negative work function/formation potential mechanism and the other was called the thermally-assisted athermal positronium. These

types of positronium are also universally observed for Si and Ge. There were several possible explanations for the formation of the two types of positronium. Considering the importance of the SiC surface as the substrate for graphene, which would be a promising target for surface positronium spectroscopy, further studies are still necessary. SiC, Si, and Ge are all indirect gap semiconductors. Positronium formation at direct gap semiconductor surfaces is an intriguing fundamental research area.

Acknowledgments

This work was financially supported by JSPS KAKENHI under Grant No. 17K19061.

ORCID iDs

A Kawasuso  <https://orcid.org/0000-0002-7065-5753>

References

- [1] Mohorovičić S 1934 *Astrono. Notes* **253** 94
- [2] Deutsch M 1951 *Phys. Rev.* **82** 455
- [3] Rubbia A 2004 *Int. J. Mod. Phys. A* **19** 3691
- [4] Karshenboim S G 2005 *Phys. Rep.* **422** 1
- [5] Shu K *et al* 2017 *J. Phys.: Conf. Ser.* **791** 012007
- [6] Ishii A 1992/93 *Solid State Phenom.* **28-29** 213
- [7] Mills A P 1993 *Positron Spectroscopy of Solids* ed A Dupasquiere and A P Mills (Amsterdam: IOS Press) p 209
- [8] Mills A P 1978 *Phys. Rev. Lett.* **41** 1828
- [9] Mills A P 1979 *Solid State Commun.* **31** 623
- [10] Nagashima Y, Morinaka Y, Kurihara T, Nagai Y, Hyodo T, Shidara T and Nakahara K 1998 *Phys. Rev. B* **58** 12676
- [11] Cassidy D B, Hisakado T H, Tom H W K and Mills A P 2011 *Phys. Rev. Lett.* **106** 133401
- [12] Cassidy D B, Hisakado T H, Tom H W K and Mills A P 2011 *Phys. Rev. B* **84** 195312
- [13] Kawasuso A, Maekawa M, Miyashita A, Wada K, Kaiwa T and Nagashima Y 2018 *Phys. Rev. B* **97** 245303
- [14] Weiss A, Jung E, Kim J H, Nangia A, Venkataraman R, Starnes S and Brauer G 1997 *Appl. Surf. Sci.* **116** 311
- [15] Brandes G R and Mills A P 1998 *Phys. Rev. B* **58** 4952
- [16] Yamashita T, Iida S, Terabe H and Nagashima Y 2016 *Nucl. Inst. Meth. Phys. Res. B* **387** 115
- [17] Marder S, Hughes V W, Wu C S and Bennett W 1956 *Phys. Rev.* **103** 1258
- [18] Lynn K G and Welch D O 1980 *Phys. Rev. B* **22** 99
- [19] Coleman P G 1992/93 *Solid State Phenom.* **28-29** 179
- [20] Wada K *et al* 2012 *Eur. Phys. J. D* **66** 37
- [21] Terabe H *et al* 2015 *Surf. Sci.* **641** 68
- [22] Cooper B S, Alonso A M, Deller A, Liskay L and Cassidy D B 2016 *Phys. Rev. B* **93** 125305
- [23] Gonze X *et al* 2002 *Comput. Mater. Sci.* **25** 478
- [24] Blöchl P E 1994 *Phys. Rev. B* **50** 17953
- [25] Perdew J P, Burke K and Ernzerhof M 1996 *Phys. Rev. Lett.* **77** 3865
- [26] Barbiellini B, Puska M J, Torsti T and Nieminen R M 1995 *Phys. Rev. B* **51** 7341(R)
- [27] Nieminen R M and Puska M J 1983 *Phys. Rev. Lett.* **50** 281
- [28] Hagiwara S, Hu C and Watanabe K 2015 *Phys. Rev. B* **91** 115409
- [29] Callewaert V *et al* 2016 *Phys. Rev. B* **94** 115411
- [30] Fazljev N G, Fry J L and Weiss A H 2004 *Phys. Rev. B* **70** 165309

- [31] Kuriplach J and Barbiellini B 2014 *Phys. Rev. B* **89** 155111
- [32] Störmer J, Goodyear A, Anwand W, Brauer G, Coleman P G and Triftshäuser W 1996 *J. Phys.: Condens. Matter* **8** L89
- [33] Ling C C, Weng H M, Beling C D and Fung S 2002 *J. Phys.: Condens. Matter* **14** 6373
- [34] Leite A M M, Debu P, Pérez P, Reymond J-M, Sacquin Y, Vallage B and Liszkay L 2017 *J. Phys.: Conf. Ser.* **791** 012005
- [35] Nangia A, Kim J H, Weiss A H and Brauer G 2002 *J. Appl. Phys.* **91** 2818
- [36] Jørgensen L V, van Veen A and Schut H 1996 *Nucl. Inst. Meth. Phys. Res. B* **119** 487
- [37] Suzuki R *et al* 1998 *Jpn. J. Appl. Phys.* **37** 4636
- [38] Britton D T, Willutzki P, Triftshäuser W, Hammerl E, Hansch W and Eisele I 1994 *Appl. Phys. A* **58** 389
- [39] Duffy J A, Bauer-Kugelmann W, Kögel G and Triftshäuser W 1997 *Appl. Surf. Sci.* **116** 241
- [40] Wiets M, Weinelt M and Fauster T 2003 *Phys. Rev. B* **68** 125321
- [41] Mattausch A and Pankratov O 2008 *Phys. Status Solidi b* **245** 1425
- [42] Emtzev K 2009 *Ph.D Thesis* Friedrich-Alexander-Universität Erlangen-Nürnberg
- [43] Sferlazzo P, Berko S, Lynn K G, Mills A P, Roellig L O, Viescas A J and West R N 1988 *Phys. Rev. Lett.* **60** 538
- [44] Iida S, Wada K, Mochizuki I, Tachibana T, Yamashita T, Hyodo T and Nagashima Y 2016 *J. Phys.: Condens. Matter* **28** 475002
- [45] Cassidy D B, Hisakado T H, Tom H W K and Mills A P 2011 *Phys. Rev. Lett.* **107** 033401
- [46] Dupasquier A 1983 *Positron Solid-State Physics* ed W Brandt and A Dupasquier (Amsterdam: North-Holland) p 510
- [47] Schultz P J and Lynn K G 1988 *Rev. Mod. Phys.* **60** 701